Research

Cytology consultations with associated image quality evaluation – experiences of the Virtual International Pathology Institute (VIPI)

Gian Kayser [1], Stephan Borkenfeld [2], Essam Ayad [3], Armina Djenouni [4], Armaz Mariamidze [5], Armen Mkhitaryan [6], Klaus Kayser [7]

[1]   Institute of Pathology, University of Freiburg, Freiburg, Germany

[2]   International Academy of Telepathology, Heidelberg, Germany

[3]   Institute of Pathology, Cairo University, Cairo, Egypt

[4]   Institute of Cytology and Pathology, Batna, Algeria

[5]   Institute of Pathology, National Cancer Center, Tblisi, Georgia

[6]   HistoGen, Armenian-German Practical Scientific Center of Pathology, Yerevan, Armenia

[7]   Institute of Pathology, Charite, Berlin, Germany

Abstract

Background: The virtual international Pathology Institute (VIPI, www.diagnomx.eu/vipi) is the only image consultation forum that is organized in close imitation to a conventional institute of pathology. Its approximately 160 experts in pathology and cytology consult and diagnose difficult cases based on a convent weekly duty plan. Herein we report the consultation results of a specific series of cytology specimens, and discuss potential application in routine virtual cytology.

Material and Methods: Still images of fine needle aspirations sent for consultation to VIPI were evaluated by five members of VIPI. A total of forty and seven cases was analyzed, and scored in four classes (benign, probably benign, probably malignant, and malignant). In addition, the consultants evaluated and graded their impression of colour, focus and general image quality in 10 classes (10 = very good <> 1 = not acceptable). Automated measurements of objective image quality, calculation of the regions of interest (ROI), and automated diagnosis classifications were performed too.

Results: The experts' diagnostic conformity was computed 4.2/5; i.e., at average 4.2 experts stated the same diagnosis of each case. The automated classification supported the summarized

experts' diagnoses in 38/47 cases. The experts interpreted the image quality diversely. Two of them evaluated with tendency of low, and two of them of high grades. The individual interactive image quality evaluations showed statistically significant relationship to the diagnostic accuracy ($p<0.05$). A helpful and correct automated ROI detection was stated in more than 95% of images.

Conclusion: The study indicates that electronic transmission of acquired conventional cytology smears is a useful tool to get access to experts' knowledge worldwide. The case related diagnostic agreement of experts can serve for gold standard of virtual cytology (for example conformity > 80%). Additional automated measurements might support the diagnosis. Implementation of virtual slide technology and automated ROI visualization are additional tools in order to support the diagnostic accuracy. Virtual international pathology institutions are able to successfully work together with or even replace conventional cytology laboratories.

Keywords: VIPI; cytology consultation, virtual diagnosis, automated measurement.

Introduction

Fine needle aspirations and their derived cytological diagnostic evaluation occupy a place close to clinical, especially radiological investigations [1-3]. In principle, it is a low risk and limited invasive, tissue – based diagnostic tool [4, 5]. In combination with gene analysis techniques and consecutive targeted therapy approaches it might probably replace more invasive methods such as biopsies in the near future [6, 7].

The morphological tools to deriving a diagnosis from cytology specimens are limited when compared to those of larger tissue specimens. Cytology structures are usually based upon intra-cellular objects such as chromatin, nucleoli, mitoses, etc. or upon small cellular agglutinations, in contrast to additional higher order structures such as glands, vessels, nerves, etc., which are present in large tissue specimens [8-10].

In history, computational analysis of cytology images focussed on the detection of 'abnormal cells', which would be suspicious for cancer [7, 11, 12]. Their automated detection is a problem of sampling, and requires a strict standardization of the underlying images [11-14]. Consecutively, precise standards of image stains and tissue preservation have been developed that focussed on Feulgen – stained smears and fine needle aspiration, in order to perform the so – called static cytometry [10, 13, 15]. At that time, an innovative server (Euroquant) was implemented [16-19]. It could be used for remote DNA cytometry, image quality evaluation, and tests of commercially available cytometry measurement systems [16-19].

Although some cytology institutes still use static DNA cytometry, the technique of Feulgen stain is widely out of use. HE, Papanicolaou and Giemsa stains are most frequently in use. Immunocytochemistry is commonly added, if needed [20].

This study focuses on reliability and reproducibility of cytological diagnosis, which might direct liquid biopsies, and assist a definitive in situ diagnosis of solid tumours. This retrospective study of several experts addresses the question 'Is the lesion benign or malignant?' In addition, it investigates in the analysis of the individual and objective image quality, automated detection of regions of interest (ROI), diagnosis performance, and a potential implementation in an electronic communication network.

Material and Methods

Cytology smears of forty and seven fine needle aspirations were uploaded to VIPI and underwent the implemented usual consultation procedure. The stains included Hematoxilin/Eosin (HE), Papanicolaou and Giemsa. Immunocytochemical investigations were not included in this study. The images were acquired with objective magnifications *10, *40. At average, 8.7 images / case have been uploaded together with the sex and age of the patients.

Five experienced experts independently classified the cases into four categories (benign, probably benign, probably malignant, malignant) as well as image quality features colour, focus, and general impression into ten different categories (1 = very poor, 10 = excellent). The percentage of agreed experts to the same diagnosis category was set (correct: >3/5; probably correct: 3/5; not applicable <3/5).

All images underwent automated quality measurements, ROI classification and feature extraction. The automated classification was added to the experts' one, and the final diagnosis category was calculated to (correct: >3/6; probably correct: 3/6; not applicable <3/6).

Image quality measurement, quantification and correction

The images were normalized for homogenous illumination (vignette), white balance (colour correction) and grey value distribution (normalization of intensity) prior to the measurements. The grey value normalization was done in the original and gradient (differentiated) image. The procedure has been described in detail elsewhere [11, 12, 21, 22]. The obtained data were statistically analyzed and correlated with the results of interactive classification.

Two different approaches were applied for ROI detection. Briefly, these included a shift array of fixed frames in 5% sizes of the whole image. They were shifted pixel by pixel over the whole image, and several features of each frame in relation to its neighbouring frames including entropy and entropy current were computed. The second approach was based upon a pixel based texture analysis. The image primitives of each grey value level were extracted, and the corresponding minimum spanning trees as well as their entropies and entropy currents were computed. The obtained maxima and minima defined the ROIs. Exemplary results are depicted in <figures 1- 3>. The whole procedure is described in detail elsewhere [14, 23, 24].
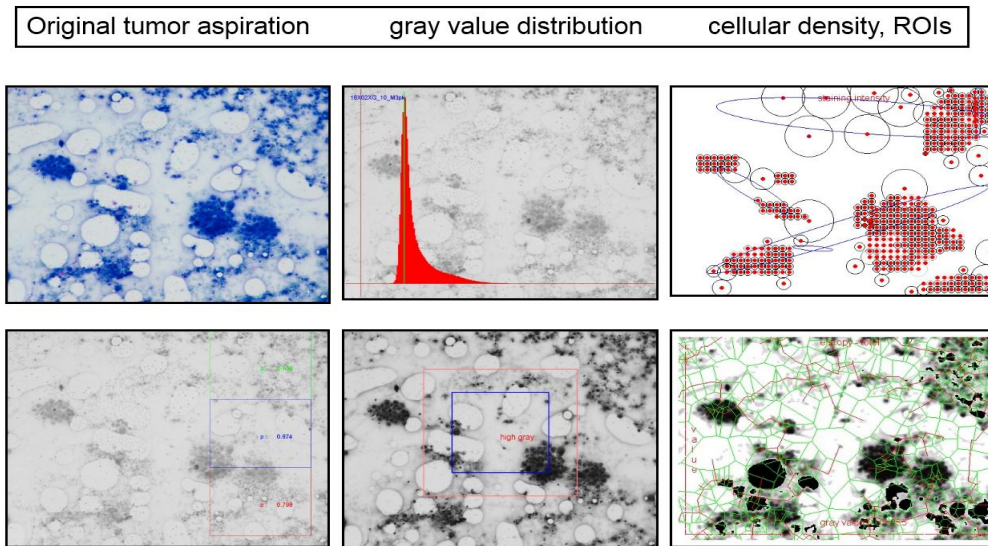
Cells and Regions of Interest (ROI)

Figure 1:   Original image of a Papanicolaou stained fine needle aspiration, grey value distribution, entropy calculations, ROI, and MST – Voronoi cells, *10.
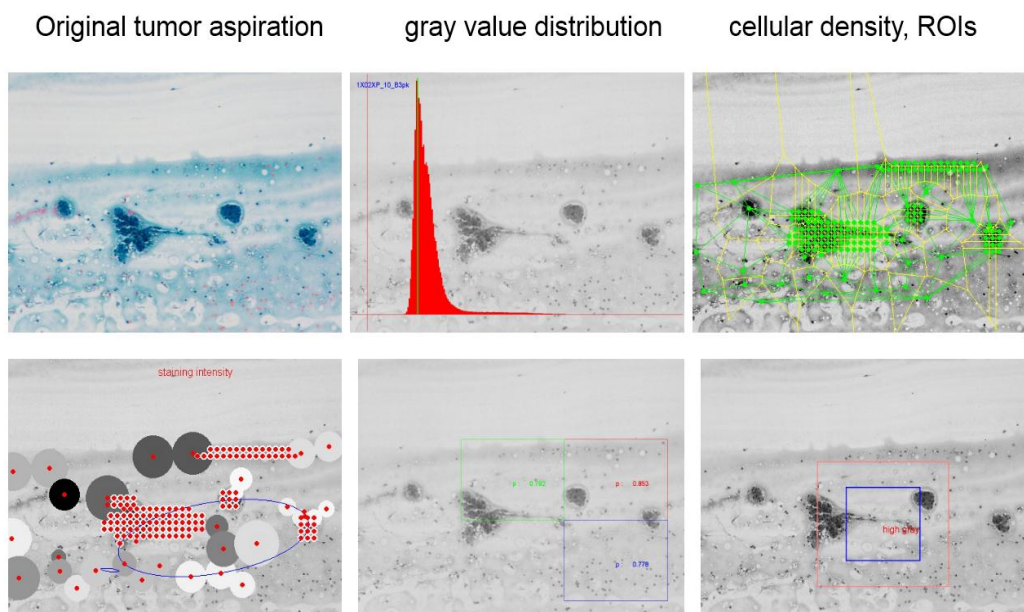
Cells and Regions of Interest (ROI) 1x2xp10b

Figure 2:   Original image of a Papanicolaou stained fine needle aspiration, grey value distribution, entropy calculations, ROI and MST – Voronoi cells. *40.

Example of ROI detection

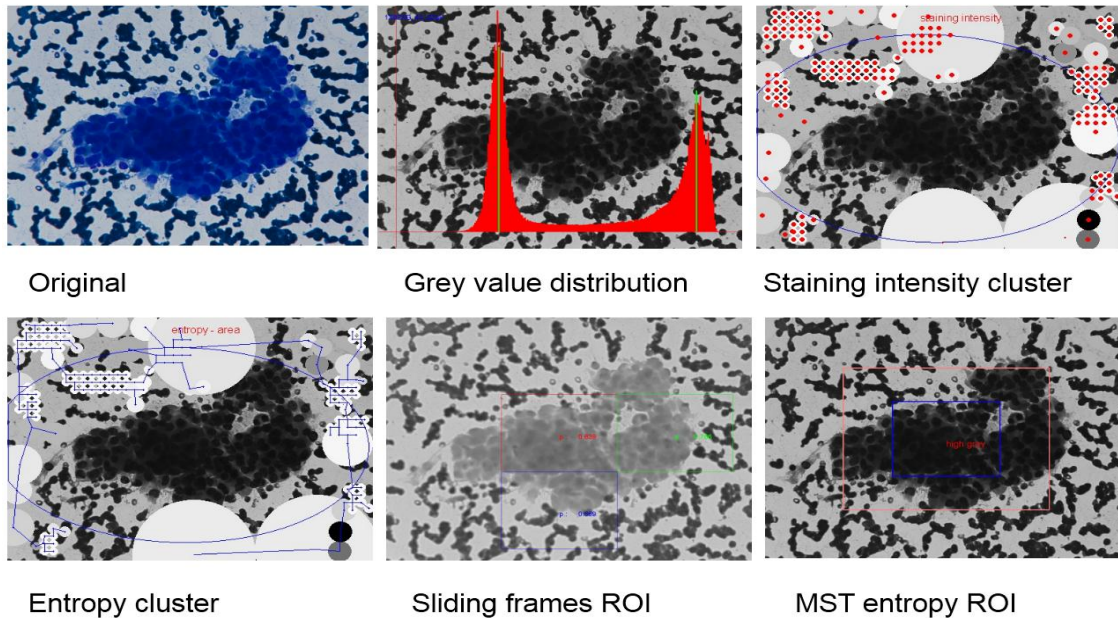| Original | Grey value distribution | Staining intensity cluster |
| Entropy cluster | Sliding frames ROI | MST entropy ROI |

Figure 3:   Example of ROI detection

The quality corrected images and their Hough, gradient and auto-regression transformations served for object (structure) and pixel (texture) related automated measurements. All images were transformed into the {hue, saturation, intensity} frame. A modified Otsu segmentation algorithm was applied to detect objects (nuclei), which were identified by features of intra-nuclear structures [25]. The entropy differences of image primitives between neighbouring grey value layers served as texture related image features. Details of the applied algorithms and results of tissue – based approaches have been described in [11, 15, 26].

The commercially available SPSS package served for statistical analysis.

Results

A total of 47 cases consisting of 20 women (mean age 65.3years) and 27 men (mean age 54.5 years) was included in the study. Five experienced experts scored 463 images, or 10 images / case at average. All five experts agreed to the same diagnosis in 27 / 47 cases. A congruent diagnosis (4/5, 5/5) was stated in 37 /47 cases, whereas a divergent diagnosis (average score < 3/5) was found in nine cases <table 1>.

The evaluation of image properties (colour, focus, general impression) differed remarkably between the experts in contrast to the results of diagnosis classification. The investigated image quality features were concordantly scored 4 – 6 by two experts in contrast to scores 8 – 9 given by two other experts, and scores 6 – 7 by one expert. All experts agreed in giving the image qualities of malignant diseases higher scores than those of benign diseases. The cases that were classified by all experts in complete agreement displayed with images of improved quality when compared to those cases which showed intra-expert disagreement or those which could not be definitely classified.

The results are presented in detail in <table 2>. Examples of original images with low and high quality scores are depicted in <Figure 4>.

Image quality assessment

A: Good, average scores 7, 8, 6

B: Moderate, average scores 5.8, 5.6, 4.8

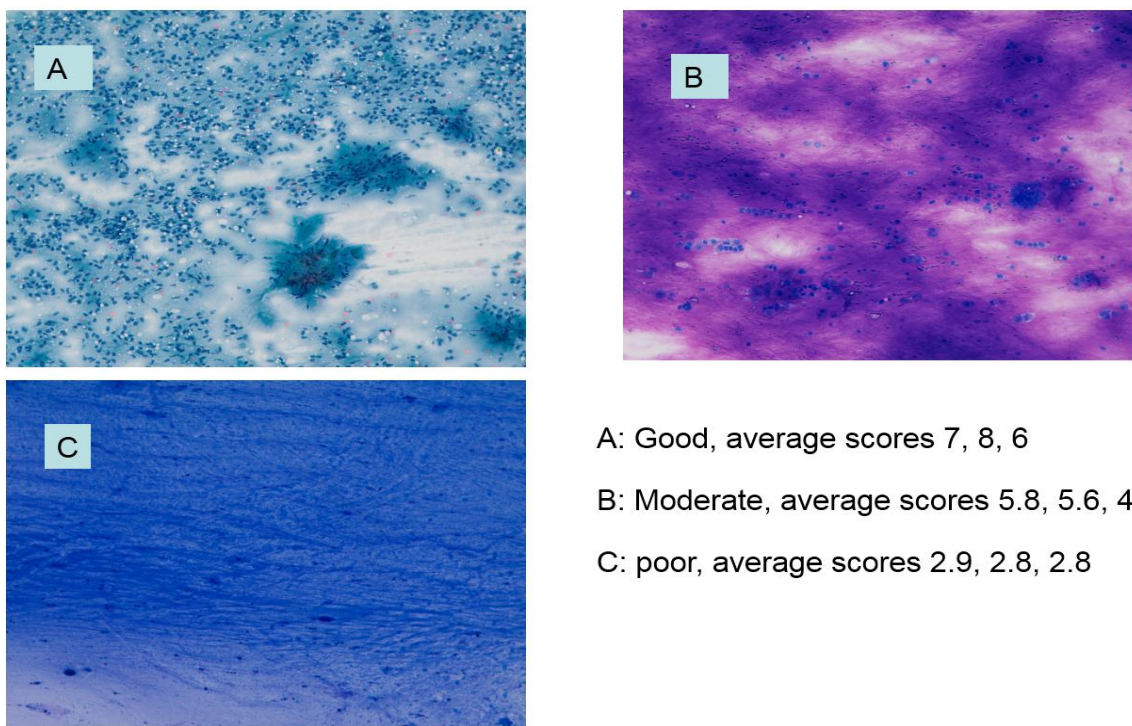C: poor, average scores 2.9, 2.8, 2.8

Figure 4:   Example of a fine needle aspiration of good, moderate, poor quality (scores 8, 5, 2.8), poor = misdiagnosed case

The accuracy of the applied automated ROI definition algorithms and the automated classification results are summarized in <table 3>. All applied algorithms are suitable to be applied in cytology. They presented with slightly improved accuracy in images of high magnification (objective *40) compared to those of low magnification (*10). The differences between the different algorithms are negligible.

Gian Kayser, Stephan Borkenfeld, Essam Ayad, Armina Djenouni, Armaz Mariamidze, Armen Mkhitaryan, Klaus Kayser;

The significant entropy features which might serve for diagnosis classification are presented in <table 4>. The automated measurements could improve the stated virtual diagnoses in 38/47 cases (<table 3>). Examples of the obtained graphs and entropy curves are depicted in <figures 5, 6>.

Entropy and segmented areas according to grey value thresholds

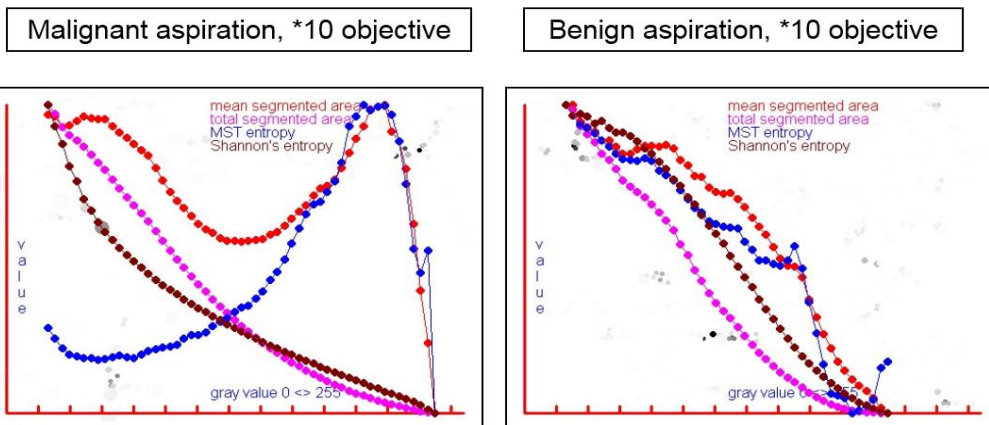# Entropy and segmented areas according to gray value thresholds

Figure 5:   Example of a fine needle aspiration showing entropy graphs and entropy current between neighbouring grey value levels of benign and malignant diseases

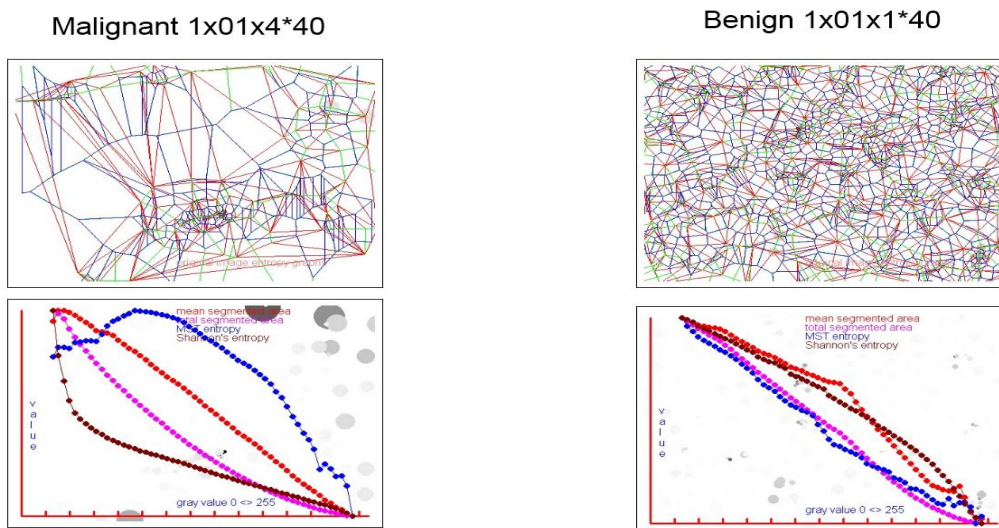# Grey value threshold graphs of benign and malignant aspirations

Figure 6:   Grey value threshold graphs of benign and malignant aspirations

9

Discussion

Telecytology or teleconsultation in cytology ranges back to the initiation of telepathology [27, 28]. For example, the first remote control server was implemented in 1995 [16-18]. It could be used for remote static DNA measurements as well as for quality evaluation of proposed stand alone measurement systems, such as MotiCyte [29]. Since that time a big step forward in image acquisition, data storage and electronic communication took place [30].

Having the technological development in mind, this study was initiated in order to answer the following questions:

Which concordance of experienced experts can be expected if a closed forum (VIPI) serves as technical tool to evaluate electronically transmitted still images?

Would the experts' diagnostic conformity be precise, and allow a potential replacement of classic cytology performance?

How diverse is an individual evaluation of image quality? Does image quality influence the diagnostic accuracy (if yes, to which degree)?

Does the individual evaluation of image quality correlate with objective image quality?

How accurate is an automated ROI positioning in cytology specimens?

Is texture analysis inferior, equal, or superior to analysis of structures and objects?

Do automated diagnostic algorithms support virtual expert consultations?

Basically, algorithms of cytology diagnostics can be separated in at least two procedures, sampling and the diagnosis itself, which includes feature extraction and classification [7, 11, 30].

The included five experts have been asked to independently state a diagnosis and to judge the quality of the uploaded images.

The interactive image interpretation and classification resulted in a high agreement of the five experts. At average, 4.2 experts agreed in their final diagnosis, and 30/47 cases were classified according to the predefined thresholds (4/5 or 5/5). This is in agreement with the reported accuracy of virtually stated cytological diagnoses in relation to conventional diagnoses [18, 20, 31, 32].

Both methods imply certain error rates, which depend upon various individual and laboratory factors. These include image quality, experts' knowledge, frequency of submitted material, etc.

10

The performance of solely virtual or classic diagnosis procedure is acceptable if both methods exhibit similar error rates. Therefore, our study indicates that distributed virtual diagnosis performance is an option for laboratories which do not posses qualified personal or which are in need of supportive actions.

Interestingly, the experts of this study have been trained and work in different countries; namely in Africa (Algeria, Egypt), Asia (Armenia, Georgia), and Europe (Germany).

The experts explored the image qualities differently, in contrast to the high diagnostic conformity. These differences apply to the average quality scores of all images, and not to those of an individual image. Images of poor quality were graded low, and those of excellent quality high by all experts; however with different absolute values. Therefore, the absolute values of image quality scores are probably induced by the experts' environment. The individual scores are probably related to the image appearance of their routine.

The average image quality scores display with a high association to the automatic measurement of colour intensity and grey value distribution of both the original and gradient images.

Thus, objective image quality measurements are a useful tool to define individual impression and quality judgement. Images of poor quality may induce wrong diagnosis statements. Image quality measurements and potential correction might serve to improving the diagnostic performance, for example, when viewing virtual slides.

Our results indicate in addition, that training can successfully replace aberrant colour and focus display. As a result, an electronically display of colours might not necessarily be adjusted to the slide colours, which are seen under the microscope [24, 33-36], because individual and objective image qualities are related to each other in diagnostic cytology approaches [24, 33-37].

Sampling applied in tissue – based diagnosis has to reliably separate objects from the background. Cytology requires in addition the detection of rare events and their separate inspection; for example tumour cells have to be distinguished from benign epithelial or inflammatory cells.

Basically, sampling procedures in cytology are time consuming. The mandatory sampling time can be successfully reduced if ROI detection algorithms are applied prior to interactive or automated diagnostic procedures [13].

Only diagnosis relevant image areas were uploaded to the VIPI forum in this study. The basic selection of adequate diagnosis relevant ROI was done interactively prior to the consultation.

The uploaded images underwent a more refined automated ROI selection after consultation. An automated determination of ROI is a prerequisite to automated diagnostic support or performance, independently from the applied algorithm [30, 38].

Even deep learning systems which might vary in their implemented algorithms commonly require standardized input images, or are seriously handicapped by numerous, often not to fulfil input events [39]. Images with small deviations from their average quality parameters such as vignette, focus, grey value distribution can be 'corrected' and standardized in relationship to the mean of all admitted images [24]. Running curves similar to those shown in <Figure 7> can visualize extremes or images that have to be excluded from measurements [30].

Image quality control running curves
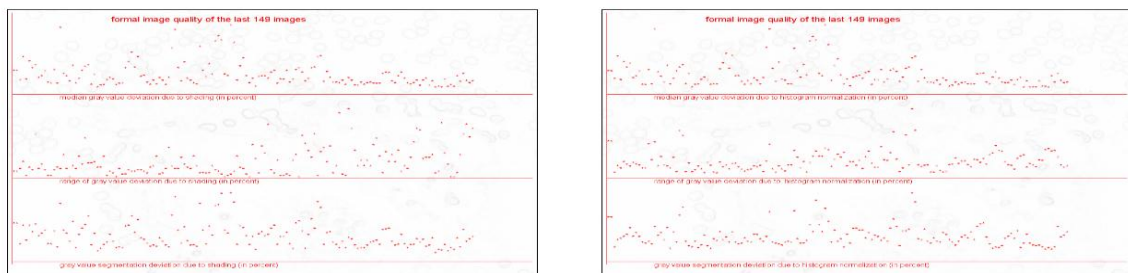

Figure 7:   Running curve of image quality measurements

Image measurements and interpretation should distinguish between extern information and image content information. Extern information defines the objects of interest, for example nuclei, cells, vessels, glands, etc. Image content information extracts the information without interpretation, for example image primitives, pixel based entropies, or grey value related features [11, 12, 15].

Having defined the nature of the objects, most algorithms measure features of the objects, for example area, circumference, grey values, moments, entropies, etc., which group them to specific object classes., The position of each object to another one, for example the nearest neighbour, most similar neighbour, etc. is an additional discrimination tool which synthesizes so – called structures.

Image content information is extracted by algorithms which do not require external information and investigate in pixel derived features [11, 12, 15]. Such an algorithm is called texture analysis.

It can be extended to detect and synthesize image primitives which can be agglutinated to intra-image 'information clusters'. These clusters can undergo similar investigations and might create several 'information layers' [7, 14].

These algorithms have been reported to reliably define ROI with high accuracy and velocity. Our results are in agreement with the results applied to tissue based measurements [22]. The accuracy is close to 100 %.

Another approach is based upon image content information too. It calculates the primitives and their entropy at each grey value level and, in addition, the entropy differences (including the entropy current between the entropies of neighbouring grey value levels).

The underlying theory proposes that in linear time relationship entropy differences are related to the velocity or strength of molecule binding of the underlying structures, [7]. The algorithm measures the functional activity instead of the structure itself, and has been successfully tested on developmental stages of chicken embryos and EGFR in breast carcinomas.

Our results indicate that image analysis of cellular functional activity might become an appropriate tool for automated detection and classification in tissue – based diagnosis including cytology.

In aggregate, several image analysis tools are ready to be applied in routine cytology diagnostics. They consist of a chain of algorithms, which start with image quality evaluation and standardization, followed by ROI detection, and finally analyze either detected objects and structures, or image primitives which are derived from textures or from functional activity.

Table 1: Survey of cases and consultation results

Total Cases	Images	Men	Women	Mean age	Mean Age
47	463	27	20	54.5	65.4

Diagnoses	correct 4/5; 5/5	probably 3/5	undefined <3/5 (agreed experts)
	30	14	3

Benign	total	definite	probably
	26	17	9

Malignant	total	definite	probably
	18	13	5

Undefined	3

Agreement of the five experts (maximum of agreed classifications)

Conformity	5 / 5	4 / 5	3 / 5	2 / 5
Cases	27	3	14	3

/

Agreement of experts and measurement classification

Conformity	complete	probably	no support
Cases	25	13	9

Table 2:   Survey of image quality evaluation

Expert	1	2	3	4	5
Color					
Diagnosis 1	4.58	7.75	7.5	4.82	7.0
Diagnosis 2	4.43	7.43	6.67	5.29	7.0
Diagnosis 3	5.64	7.33	5.73	5.58	7.56
Diagnosis 4	5.56	9.0	8.64	5.33	8.67
Mean	5.05	7.88	7.14	5.26	7.557
Focus					
Diagnosis 1	5.0	7.15	7.06	4.47	6.82
Diagnosis 2	5.29	6.47	6.0	4.43	7.0
Diagnosis 3	5.18	6.67	5.0	4.83	7.44
Diagnosis 4	5.67	8.30	7.91	5.33	8.0
Mean	5.285	7.15	6.49	4.765	7.32
General Quality					
Diagnosis 1	4.47	7.5	7.17	4.76	6.12
Diagnosis 2	4.0	6.14	6.60	4.86	6.44
Diagnosis 3	5.18	7.33	5.0	5.0	7.56
Diagnosis 4	5.78	8.90	8.36	5.22	7.73
Mean	4.86	7.47	6.78	4.96	6.96

Table 3:   Entropy diagnosis classification and accuracy of automated ROI

47 cases, 463 images (x10, x40, objective); diagnosis classification according to the relative number of identical classified images per cases

Classified cases (only entropy curves, images / case)

- All images identical: 23 cases   definite support
- >50% images identical: 18 cases   probable support
- <50 % images identical: 6 cases   no support (non defined)

- Experts' statement and measurement support:

	Experts	Increased probability by measurements	
Probably benign	9	3	(indicating benign)
Probably malignant	5	1	(indicating malignant)
Undefined	3	1	(indicating benign)

Table 4: Significant entropy features (useful in deep learning / multivariate statistical discrimination analysis)

Algorithms	Benign	Malignant
Entropies		
• MST (image primitives):	0.350	0.424 **)
• Shannon (image primitives):	6.050	5.421 *)
• MST (object related):	3.179	3.855 **)
• Shannon (object related):	6.317	6.060 *)
Entropy flows		
• Recursive (image primitives):	0.259	0.247
• Shannon (image primitives):	0.108	0.144 **)
• Shannon recursive maximum:	1.249	1.610 **)
• Shannon recursive minimum:	0.169	0.208 **)

Significance levels: *) $p<0.05$; **) $p<0.01$

References

1. Hang JF, Shum CH, Ali SZ, Bishop JA. Cytological features of the Warthin-like variant of salivary mucoepidermoid carcinoma. Diagn Cytopathol. 10.1002/dc.23785.

2. Krishna SG, Rao BB, Ugbarugba E, Shah ZK, Blaszczak A, Hinton A, Conwell DL, Hart PA. Diagnostic performance of endoscopic ultrasound for detection of pancreatic malignancy following an indeterminate multidetector CT scan: a systemic review and meta-analysis. Surg Endosc.

3. Marco Sperandeo, Francesca Maria Trovato, Nadia Melillo, Lucia Dimitri, Giuseppe Musumeci, Giuseppe Guglielmi. The role of ultrasound-guided fine needle aspiration biopsy in musculoskeletal diseases. Eur J Radiol. 90: p. 234-244.

4. Feride Fatma Görgülü, Fatma Yasemin Öksüzler, Süheyla Aytaç Arslan, Muhammet Arslan, İbrahim Ethem Özsoy, Orhan Görgülü. Computed tomography-guided transthoracic biopsy: Factors influencing diagnostic and complication rates. J Int Med Res. 45(2): p. 808-815.

5. Hong MJ, Na DG, Baek JH, Sung JY, Kim JH. Cytology-Ultrasonography Risk-Stratification Scoring System Based on Fine-Needle Aspiration Cytology and the Korean-Thyroid Imaging Reporting and Data System. Thyroid. 27(7): p. 953-959.

6. A L Mitchell, A Gandhi, D Scott-Coombes, P Perros. Management of thyroid cancer: United Kingdom National Multidisciplinary Guidelines. J Laryngol Otol. 130(S2): p. S150-S160.

7. Kayser G, Görtler J, Weis CA, Borkenfeld S, Kayser K. The application of structural entropy in tissue based diagnosis. Diagnostic Pathology, 2017. 3(1).

8. Kayser G, Baumhäkel JD, Szöke T, Trojan I, Riede U, Werner M, Kayser K. Vascular diffusion density and survival of patients with primary lung carcinomas. Virchows Arch, 2003.

9. Kayser K, Gabius HJ. The application of thermodynamic principles to histochemical and morphometric tissue research: principles and practical outline with focus on the glycosciences. Cell Tissue Res, 1999. 296(3): p. 443-55.

10. Kayser K, Liewald F, Kremer K, Tacke M. Integrated optical density (IOD), syntactic structure analysis, and survival in operated lung carcinoma patients. Pathol Res Pract, 1994. 190(11): p. 1031-8.

11.   Kayser K1, Hoshang SA, Metze K, Goldmann T, Vollmer E, Radziszowski D, Kosjerina Z, Mireskandari M, Kayser G. Texture- and object-related automated information analysis in histological still images of various organs. Anal Quant Cytol Histol, 2008. 30(6): p. 323-35.

12.   Kayser K, Kayser G, Metze K. The concept of structural entropy in tissue-based diagnosis. Anal Quant Cytol Histol, 2007. 29(5): p. 296-308.

13.   Kayser K, Baumgartner K, Gabius HJ. Cytometry with DAPI-stained tumor imprints. A reliable tool for improved intraoperative analysis of lung neoplasms. Anal Quant Cytol Histol, 1996. 18(2): p. 115-20.

14.   Kayser K, Berthold S, Eichhorn S, Kayser C, Ziehms S, Gabius HJ. Application of attributed graphs in diagnostic pathology. Anal Quant Cytol Histol, 1996. 18(4): p. 286-92.

15.   Kayser K, Stute H, Bubenzer J, Paul J. Combined morphometrical and syntactic structure analysis as tools for histomorphological insight into human lung carcinoma growth. Anal Cell Pathol, 1990. 2(3): p. 167-78.

16.   Haroske G, Meyer W, Oberholzer M, Böcking A, Kunze KD. Competence on demand in DNA image cytometry. Pathol Res Pract, 2000. 196(5): p. 285-91.

17.   Haroske G, Meyer W, Theissig F, Schubert K, Kunze KD. Remote quantitation server for quality assurance in DNA ploidy analysis. Anal Quant Cytol Histol, 1998. 20(4): p. 302-12.

18.   Kayser K, Blum S, Beyer M, Haroske G, Kunze KD, Meyer W. Routine DNA cytometry of benign and malignant pleural effusions by means of the remote quantitation server Euroquant: a prospective study. J Clin Pathol, 2000. 53(10): p. 760-4.

19.   Kayser K, Kayser G, Radziszowski D, Oehmann A. New developments in digital pathology: from telepathology to virtual pathology laboratory. Stud Health Technol Inform, 2004. 105: p. 61-9.

20.   Schmitt F. Telepathology devoted to cytology. Diagnostic Pathology, 2017. ECP 2017 SY_03_1.

21.   Kayser K, Jacinto SD, Böhm G, Frits P, Kunze WP, Nehrlich A, Gabius HJ. Application of computer-assisted morphometry to the analysis of prenatal development of human lung. Anat Histol Embryol, 1997. 26(2): p. 135-9.

22.   Görtler J, Kayser K, Borkenfeld S, Carvalho R, Kayser G. Cognitive Algorithms and digitized Tissue – based Diagnosis. Diagnostic Pathology, 2017. 3(1).

23.   Kayser K, Becker C, Seeberg N, Gabius HJ. Quantitation of asbestos and asbestos-like fibers in human lung tissue by hot and wet ashing, and the significance of their presence for survival of lung carcinoma and mesothelioma patients. Lung Cancer, 1999. 24(2): p. 89-98.

24.   Kayser K, Görtler J, Metze K, Goldmann T, Vollmer E, Mireskandari M, Kosjerina Z, Kayser G. How to measure image quality in tissue-based diagnosis (diagnostic surgical pathology). Diagn Pathol, 2008. 3 Suppl 1: p. S11.

25.   Otsu, N., A threshold selection method from grey level histograms. IEEE Transactions on Systems, Man, and Cybernetics. 1979. 9: p. 62-66.

26.   Kayser K, Richter B, Stryciak R, Gabius HJ. Parameters derived from integrated nuclear fluorescence, syntactic structure analysis, and vascularization in human lung carcinomas. Anal Cell Pathol, 1997. 15(2): p. 73-83.

27.   Leong FJ, Leong AS. Digital photography in anatomical pathology. J Postgrad Med, 2004. 50(1): p. 62-9.

28.   Marsan C, Vacher-Lavenu MC. Telepathology: a tool to aid in diagnosis and quality assurance in cervicovaginal cytology. Cytopathology, 1995. 6(5): p. 339-42.

29. www.moticeurope.com/newsletter/2014/02february/moticnews_february_2014_de.html.

30.   Kayser K, Molnar B, Weinstein RS. *Virtual Microscopy Fundamentals - Applications - Perspectives of Electronic Tissue - based Diagnosis*. 2006, Berlin: VSV Interdisciplinary Medical Publishing.

31.   Collins BT. Telepathology in cytopathology: challenges and opportunities. Acta Cytol. 57(3): p. 221-32.

32.   Thrall MJ, Wimmer JL, Schwartz MR. Validation of multiple whole slide imaging scanners based on the guideline from the College of American Pathologists Pathology and Laboratory Quality Center. Arch Pathol Lab Med. 139(5): p. 656-64.

33.   Higgins C. Applications and challenges of digital pathology and whole slide imaging. Biotech Histochem. 90(5): p. 341-7.

34.   Krupinski EA, Silverstein LD, Hashmi SF, Graham AR, Weinstein RS, Roehrig H. Observer performance using virtual pathology slides: impact of LCD color reproduction accuracy. J Digit Imaging. 25(6): p. 738-43.

35.   Lin DY, Blumenkranz MS, Brothers RJ, Grosvenor DM. The sensitivity and specificity of single-field nonmydriatic monochromatic digital fundus photography with remote image interpretation for diabetic retinopathy screening: a comparison with

ophthalmoscopy and standardized mydriatic color photography. Am J Ophthalmol, 2002. 134(2): p. 204-13.

36. Smith AC, Kimble R, Mill J, Bailey D, O'Rourke P, Wootton R. Diagnostic accuracy of and patient satisfaction with telemedicine for the follow-up of paediatric burns patients. J Telemed Telecare, 2004. 10(4): p. 193-8.

37. Bautista PA, Yagi Y. Improving the visualization and detection of tissue folds in whole slide images through color enhancement. J Pathol Inform. 1: p. 25.

38. Ayad E, Borkenfeld S, Djenouni A, Kayser K, Kayser G. Cytology consultations with associated image quality evaluation and image measurements. Diagnostic Pathology, 2017. 3(ECP 2017 SY-03).

39. Litjens G, Kooi T, Bejnordi BE, Setio AAA, Ciompi F, Ghafoorian M, van der Laak JAWM, van Ginneken B, Sánchez CI. A survey on deep learning in medical image analysis. Med Image Anal. 2017 42:60-88.